HHS Public Access

Author manuscript

Gastroenterology. Author manuscript; available in PMC 2016 July 06.

Published in final edited form as:

Gastroenterology. 2011 September ; 141(3): 819–826.e1. doi:10.1053/j.gastro.2011.07.027.

Ultrasound Elasticity Imaging for Detecting Intestinal Fibrosis and Inflammation in Rats and Humans With Crohn's Disease

Ryan W. Stidham[*], **Jingping Xu**[‡,§], **Laura A. Johnson**[*], **Kang Kim**[‡,§,‖], **David S. Moons**[¶], **Barbara J. Mckenna**[¶], **Jonathan M. Rubin**[#], and **Peter D. R. Higgins**[*]

[*]Department of Medicine, University of Michigan, Ann Arbor, Michigan

[‡]Center for Ultrasound Molecular Imaging and Therapeutics, University of Pittsburgh Medical Center, Pittsburgh, Pennsylvania

[§]Cardiovascular Institute, University of Pittsburgh Medical Center, Pittsburgh, Pennsylvania

[‖]Department of Bioengineering, University of Pittsburgh, Pittsburgh, Pennsylvania

[¶]Department of Pathology, University of Michigan, Ann Arbor, Michigan

[#]Department of Radiology, University of Michigan, Ann Arbor, Michigan

Abstract

BACKGROUND—Intestinal fibrosis causes many complications of Crohn's disease (CD). Available biomarkers and imaging modalities lack sufficient accuracy to distinguish intestinal inflammation from fibrosis. Transcutaneous ultrasound elasticity imaging (UEI) is a promising, noninvasive approach for measuring tissue mechanical properties. We hypothesized that UEI could differentiate inflammatory from fibrotic bowel wall changes in both animal models of colitis and humans with CD.

METHODS—Female Lewis rats underwent weekly trinitrobenzene sulfonic acid enemas yielding models of acute inflammatory colitis (n = 5) and chronic intestinal fibrosis (n = 6). UEI scanning used a novel speckle-tracking algorithm to estimate tissue strain. Resected bowel segments were evaluated for evidence of inflammation and fibrosis. Seven consecutive patients with stenotic CD were studied with UEI and their resected stenotic and normal bowel segments were evaluated by ex vivo elastometry and histopathology.

RESULTS—Transcutaneous UEI normalized strain was able to differentiate acutely inflamed (−2.07) versus chronic fibrotic (−1.10) colon in rat models of inflammatory bowel disease (IBD; P = .037). Transcutaneous UEI normalized strain also differentiated stenotic (−0.87) versus adjacent normal small bowel (−1.99) in human CD (P = .0008), and this measurement also correlated well with ex vivo elastometry (r = −0.81).

Address requests for reprints to: Peter D.R. Higgins, SPC 5682, 1150 West Medical Center Drive, Ann Arbor, Michigan 48109. phiggins@umich.edu.

Supplementary Material

Note: To access the supplementary material accompanying this article, visit the online version of *Gastroenterology* at www.gastrojournal.org, and at doi:10.1053/j.gastro.2011.07.027.

Conflicts of interest

The authors disclose no conflicts.

CONCLUSIONS—UEI can differentiate inflammatory from fibrotic intestine in rat models of IBD and can differentiate between fibrotic and unaffected intestine in a pilot study in humans with CD. UEI represents a novel technology with potential to become a new objective measure of progression of intestinal fibrosis. Prospective clinical studies in CD are needed.

Keywords

Ultrasound; Fibrosis; Crohn's Disease; Elastography

Intestinal fibrosis and subsequent stricturing of the intestine in Crohn's disease (CD) result in substantial patient morbidity and mortality.[1] Fibrostenotic complications are responsible for a significant proportion of hospitalizations, surgeries, and health care costs of CD.[2,3] Immunosuppressive therapies are often successful in treating inflammation in CD, but fail to address preexisting intestinal fibrosis.[4,5] Advances in imaging technology, including computerized tomographic enterography and magnetic resonance enterography, have improved the assessment of CD extent and activity. However, neither imaging techniques nor blood testing can reliably distinguish fibrotic from inflammatory strictures. Stricture management is a common clinical dilemma; inflammatory strictures are likely to respond to intensification of medical therapy, but symptomatic fibrotic strictures often require operative intervention. Symptomatic, noncritical stenoses are often repeatedly treated with trials of immunosuppressive therapy with little benefit, despite known risks and side effects. Knowledge of stricture composition could aid stricture management, driving medical intensification for inflammation and hastening symptomatic recovery, or limiting exposure to futile, potentially harmful medical therapies by providing an objective indication for operative intervention.

Ultrasound elasticity imaging (UEI) noninvasively assesses tissue mechanical properties by measuring strain that is developed in the tissue. Strain is the degree of compression of a material in response to a force applied to a fixed area (stress). Materials exhibiting low strain in response to a fixed stress have less compliance, and are commonly described as stiffer or harder. UEI estimates strain by ultrasound speckle tracking.[6,7] UEI has been applied successfully to other human disease states, including differentiating acute versus chronic deep venous thrombosis,[8,9] identifying diastolic heart failure with cardiac elasticity imaging,[10] and differentiating acute rejection versus healthy kidney in renal transplants.[11]

Prior work by our group has demonstrated that UEI can identify intestinal fibrosis in animal models of CD.[12] UEI strain estimates have clearly differentiated abnormal bowel in trinitrobenzene sulfonic acid (TNBS)-treated Lewis rats from normal bowel in the same animal. UEI strain data correlated well to direct mechanical measurement of the tissue elastic properties and histology analysis of these ex vivo specimens. These results suggested that UEI detection of decreased tissue strain is an accurate surrogate marker for intestinal fibrosis. In this study, we have investigated the ability of intestinal UEI to identify the presence and extent of diseased bowel in rats, and to distinguish bowel wall thickening owing to predominantly inflammatory versus fibrotic changes. In addition, we applied the UEI technique for the investigation of strictures in CD before elective operative resection, and compared the results of UEI with mechanical measurement and histopathology.

Methods

Animal Models of Acute Colitis and Intestinal Fibrosis

Acute colitis and colonic fibrosis were generated in Lewis rats by rectal administration of TNBS enemas, a well-accepted model of colitis developed by Morris et al.[13] A total of 15 female Lewis rats (Harlan Sprague–Dawley; Harlan, Indianapolis, IN; weight, 150–180 g) were separated into 3 groups: Acute colitis, chronic intestinal fibrosis, and phosphate-buffered saline (PBS) enema negative controls; 1 rat in the acute colitis group did not survive treatment. Rodents were fasted for 16–24 hours and provided with free access to an iso-osmotic bowel preparation (GoLytely PEG-3350, Braintree Labs, Braintree, MA), to eliminate colonic stool before catheter insertion for TNBS enemas. Rats were anesthetized with vaporized isoflurane using the drop jar technique. Enemas were administered by placing sedated rodents in a head-down position, inserting a 5-French neonatal feeding tube 6 cm into the rectum, and slowly instilling 250 μL of either TNBS solution or a control solution of PBS. The enema tube remained in place for 60 seconds to ensure adequate delivery to the distal colon.

The intestinal fibrosis group received weekly enemas, consisting of TNBS-50% ethanol in a total volume of 250 μL, with escalating weekly TNBS doses over 6 weeks of treatment with 15, 30, 45, 60, 60, and 60 mg TNBS over the course of the experiment. This group was rested 7–10 days before UEI scans and killed to allow resolution of acute inflammation from the final enema. The acute colitis group received a single 50% ethanol enema with 15 mg of TNBS; these animals were analyzed by UEI and killed 48–72 hours after enemas so that studies would capture acute inflammatory changes in the colon. Negative control animals received 250 μL PBS enemas in identical fashion to the TNBS animals, weekly for 6 weeks.

During the weekly treatment phase, animals were monitored for health indicators, including weight, stool blood, diarrhea, and general activity. After UEI measurement, animals were killed by CO_2 inhalation, after which the colon was resected, opened longitudinally, and stool was removed. Colon weight and length were measured, and the colon was photographed after gross assessment for ulceration, necrosis, and fibrosis. Distal (treated) and proximal (unaffected) sections of colon tissue were resected for histology, protein analysis, and mechanical property measurement. Gross effects of treatment enemas were limited to the distal colon, where enemas were delivered. The protocol was approved by the University of Michigan Committee on the Use and Care of Animals and strictly complied with National Institutes of Health Guide for Care and Use of Laboratory Animals.

UEI Strain Measurement in Rodents

At completion of treatment, rodents underwent abdominal ultrasound, immediately followed by euthanasia for ex vivo biologic analysis of the colon. Standard ultrasound B-scan images and ultrasound radiofrequency (RF) data were collected using a commercially available ultrasound scanner (Z-1, Zonare Medical Systems, Mountain View, CA) and standard linear array transducer centered at 6.8 MHz, capturing 458 frames at 75 Hz, at a depth of 25–35 mm. Before ultrasound analysis, rodents were anesthetized with ketamine (36 mg/kg) and xylazine (3.6 mg/kg). After abdominal fur shaving and application of ultrasound gel,

animals were placed supine on a custom-built platform below the ultrasound transducer. The transducer was fixed to a crank arm, allowing uniform pressure and displacement to be applied during the 6-second abdominal deformation. Before deformation, the animals were aligned by centering the ultrasound image over the pubis symphysis, whose inverted "U" structure was readily identified. After alignment, a mild preload force was exerted on the abdomen cephalad to the pubis symphysis in the transverse plane to push away luminal stool and gas, and reduce shadowing artifacts. Mild preload force does not affect elastic properties of the colon wall. Steady cranking of the transducer toward the abdomen over 6 seconds deformed and compressed the collapsed bowel wall of proximal and distal treated colon, and RF ultrasound data were captured during the deformation. Proximal colon could easily be identified separate from the treated distal colon based on its anatomic location.

Human Subjects Undergoing UEI

The Institutional Review Board of the University of Michigan approved the study protocol and all participants provided signed informed consent before participating in the study. CD patients scheduled for elective resection of symptomatic small bowel strictures (n = 7) were enrolled. Human subjects underwent transabdominal ultrasound using the same ultrasound machine utilized in the animal experiments. Strictures were readily identified in all patients, because investigators utilized existing cross-sectional imaging results, including computed tomography and magnetic resonance imaging, to guide ultrasound evaluation of the strictures. Upon stricture identification, an ultrasound window including the thickened stricture and a loop of ultrasonographically normal bowel were acquired. The crankshaft used to standardize rat luminal deformations was not used in humans, because bowel wall deformations were performed freehand. RF images were captured at 75 Hz over a 6-second bowel deformation, using the transducer to apply abdominal pressure. All scans were performed within 2 days before surgery (mean. 0.7; median, 0; range, 0–2). Immediately after operative resection, the resected section of stenotic bowel was placed in isotonic saline and sections were taken from representative portions of both stricture and grossly normal tissue for histology and immediate mechanical measurements, as described.

Statistical Analysis

Comparisons between treatment groups were performed using a paired 2-tailed *t* test. A difference of the means with $P < .05$ was considered significant. Additional methods describing the histopathologic analysis, immunoblotting, ultrasound image processing, and direct mechanical measurements of tissue stiffness are reported in the Supplementary Methods section.

Results

Acute TNBS Enemas Induce Inflammatory Colitis, Whereas Chronic TNBS Enemas Induce Colonic Fibrosis in Rats

The objective of the animal portion of our study was to determine whether UEI measurements of the rat colon could distinguish inflammatory and fibrotic causes of bowel wall thickening. Biologic confirmation of the fibrotic and inflammatory phenotypes was performed by gross pathologic, histologic, and molecular methods. At sacrifice, gross colon

morphology was consistent with inflammation and fibrosis (Figure 1*A*). The acute TNBS colitis group demonstrated distal colon thickening with areas of hemorrhagic necrosis and a subjectively soft texture. The chronic TNBS group also had distal colon thickening, but its texture was hard and rigid. The chronic TNBS group colon length was shorter compared with the control and inflammation groups. The distal colon of control animals that received PBS enemas was grossly unremarkable. Gross pathologic effects were limited to the extent of TNBS instillation in the distal colon; the proximal colon was normal in all rat groups. Colon density (mass/length), was significantly greater in the chronic fibrosis rat group (0.24 ± 0.065 g/cm), compared with the acute TNBS-colitis model (0.18 ± 0.018 g/cm; $P = .047$; data not shown). Although the chronic fibrosis group's normalized colon weight differed from PBS-control rats (0.16 ± 0.045 g/cm; $P = .006$), the average acute TNBS-colitis rat colon tissue weight did not significantly differ from the controls.

Histologic review of tissue sections from distal colon in acute and chronically TNBS-treated animal groups revealed changes indicative of acute colitis and intestinal fibrosis phenotypes, respectively (Figure 1*B*). Thickening of the mucosa and submucosa was evident in both the groups. However, Masson's trichrome staining showed substantially more collagen deposition in the chronic fibrosis group, whereas mucosal thickening in the acute inflammatory group was associated with edema and an inflammatory cellular infiltrate with little change in collagen distribution. An inflammatory infiltrate was present in both TNBS rat groups, but was more prominent in the acute inflammatory group. Mucosal ulceration was present in both the acute inflammatory and the chronic fibrosis groups, but only the acute group demonstrated patchy regions of necrosis. Finally, substantial thickening of the muscularis mucosa was revealed by α-smooth muscle actin (α-SMA) staining and prominent architectural distortion in the chronic fibrosis group. In summary, acute and chronic TNBS treatment of the rat distal colon consistently produced phenotypes consistent with acute colitis and chronic intestinal fibrosis in the rat distal colon, whereas the proximal colon remained unaffected (Figure 1*C*). Overall, chronic fibrosis rats demonstrated histologic changes comparable with human fibrostenotic strictures in inflammatory bowel disease (IBD), whereas the acute inflammatory group showed characteristics of acute colitis without fibrotic changes.

Western blotting for α-SMA, a marker of tissue fibrosis, was dramatically induced in the chronic fibrosis group compared with both PBS controls and acute colitis groups, suggesting that activation of myofibroblast fibro-genesis in the chronic fibrotic model compared with the acute inflammatory model and PBS control rats (Figure 1*D*). In summary, chronic fibrosis rats demonstrated greater colonic mass and density as well as histopathology and protein expression characteristic of human fibrostenotic strictures.

UEI Strain Measurement Distinguishes Inflammatory From Fibrotic Thickened Colon in TNBS-Treated Rats

Proximal and distal segments of colon were identified in anesthetized rats by transabdominal ultrasound. Distal colon segments from inflamed and fibrotic groups exhibited wall thickening compared with their proximal colons, and to the distal colons of negative control rats. UEI was used to measure the bowel wall strain in distal (affected) and proximal

(unaffected) colon (Figure 2*A*). Low strain values indicate hard tissue with limited deformation; high strain indicates soft, deformable tissue. Mean UEI normalized strain was lowest (hardest) in the distal colon of the chronic fibrosis group (−1.10 ± 0.167), highest (softest) in the distal colon of the negative controls (−3.57 ± 0.352), and an intermediate mean strain was found in the acute inflammation group (−2.07 ± 0.717; Figure 2*B*). The UEI normalized strain differed between the negative control group and the acute inflammation group ($P = .015$), and also between the negative control group and the chronic fibrosis group ($P = .001$). A significant difference in UEI strain was also found between the acute inflammation and chronic fibrosis groups ($P = .037$), given the possible variation in both transabdominal force applied and individual rat anatomy. The UEI strain ratio in the chronic fibrosis group measured −0.43 ± 0.09; the PBS-negative control group was −0.87 ± 0.07, and it was −0.54 ± 0.09 in the acute inflammation group. The UEI strain ratio differed significantly between the chronic fibrosis and the acute inflammation groups ($P = .030$).

Direct Measurement of Colon Mechanical Properties Correlates With UEI Strain in Rats

UEI strain noninvasively measures the mechanical properties of tissue. Microelastometer measurements of ex vivo colon tissue samples measure the stress–strain relationship of the tissue, and the slope of this curve represents Young's Modulus of the tissue (YM). High YM indicates rigidity, or hardness; it is, therefore, inversely correlated with strain. Stress–strain curves of the distal colon samples from all rat groups demonstrated that YM was highest (2.75 ± 0.56 kPa; hardest) in chronic fibrosis group, lowest (0.30 ± 0.25 kPa; softest) in the PBS-negative control group, and intermediate (2.16 ± 0.40 kPa) in the acute inflammation group (Figure 2*C*). Proximal colon measurements were similar across groups with a mean YM of 0.92 kPa (range, 0.49 –1.15). The mean normalized YM ratio (distal divided by proximal colon YM) for chronic fibrosis, acute inflammation, and PBS-negative control groups were 6.57, 3.07, and 1.18, respectively. All differences between these 3 groups were significant (fibrosis vs inflammatory, $P = .024$; inflammatory vs control, $P = .042$; fibrosis vs control, $P = .035$).

UEI Strain Measurement Distinguishes Normal Bowel From Fibrotic Bowel in Human Subjects With CD

Preoperative transcutaneous ultrasound scans were performed in 7 human subjects using the same ultrasound device and 2-dimensional speckle tracking algorithms as in the rat experiments. In human subjects, the scanning plane included both diseased stenotic bowel and an adjacent loop of ultrasonographically unaffected small intestine (with a nonthickened bowel wall). Deformation using the scanning transducer was performed manually on supine patients, and off-line image processing was used to generate UEI strain maps (Figure 3*A*). UEI-normalized strain values were lower (harder) in stenotic bowel, with a mean normalized strain of −0.87 ± 0.22, whereas adjacent normal bowel strain averaged −1.99 ± 0.53 ($P = .0008$). Strain was only compared between normal and stenotic bowel within individual human cases given the necessity of operative specimens in this pilot study.

Direct Measurement of the Mechanical and Biologic Properties of Ex Vivo Small Bowel Tissue Samples Correlated With UEI Strain in Human Small Intestine

Tissue from stenotic and adjacent normal-appearing small bowel resection margins underwent immediate direct measurement of tissue mechanical properties using the tissue elastometer. The YM in stenotic tissue was significantly harder (mean 4.14 ± 1.88 kPa) than that of the (grossly normal) tissue from the surgical resection margin (mean 0.96 ± 0.25 kPa; $P = .0009$; Figure 3*C*, *left panel*). Variability of stiffness in the stenotic tissue was expected resulting from differences in biologic disease severity, unavoidable variation in specimen sectioning, and heterogeneity of stiffness within the section itself. The UEI strain was inversely correlated by Pearson's coefficient with the direct measurements of YM ($r = -0.81$; Figure 3*C*, *right panel*). As in the TNBS rats, noninvasive transcutaneous measurement of tissue strain by UEI accurately measured the ex vivo mechanical properties of the resected small intestine in CD.

Histology assessment of ex vivo stenotic and grossly normal small bowel margins confirmed that the strictures were predominantly fibrotic, and the grossly normal resection margins lacked major inflammatory or fibrotic changes (Figure 3*B*). Stenotic tissue demonstrated significant architectural distortion, mucosal and submucosal expansion, and evidence of submucosal collagen deposition. The stenotic tissue was not purely fibrotic, containing mild and occasionally moderate inflammatory cellular infiltrates. In addition, some resection margins of grossly normal tissue demonstrated mild inflammatory changes, possibly harboring active IBD, but no evidence of fibrosis was found in these samples. By pathologic grading, all of the stenotic tissue samples demonstrated severe fibrotic changes while normal tissue displayed no fibrosis and minimal inflammatory changes.

Discussion

The monitoring and management of inflammation in IBD have undergone revolutionary advances in the past 20 years, but the development of methods of detection and treatment of fibrosis in CD have lagged behind. Fibrostenotic complications lead to frequent hospital admissions, operative interventions, and substantial costs in CD. At present, our armamentarium against fibrosis is limited to preventive, anti-inflammatory strategies. Anti-fibrotic therapies for other organs may hold promise for intestinal fibrosis. A means to identify and quantify intestinal fibrosis in vivo would represent a new physiologic surrogate end point in the monitoring of chronic CD.

Our previous proof-of-concept study demonstrated that (1) the mechanical properties of intestine can distinguish normal from fibrotic intestine in a chronic TNBS rat model of IBD, and (2) noninvasive transcutaneous UEI can reliably detect changes in tissue mechanical stiffness.[12] In this translational study, we found that UEI could differentiate inflammatory from fibrotic intestine in TNBS rat models of IBD, that UEI is feasible in humans, and that transcutaneous UEI accurately measures the tissue properties of stenotic segments of the bowel in patients with CD when compared with the gold standard of tissue elastometry.

There are several limitations to this study. UEI was performed by a single expert ultrasonographer (J.R.). Ultrasonography is well established for the evaluation of CD in

expert centers in Europe, but it is not clear how readily generalizable this approach is to community practice.[14] However, published studies of interobserver agreement in ultrasound for CD have found satisfactory to excellent reproducibility when reporting was standardized.[15] The current interpretation of the RF speckle tracking data requires off-line processing with specialized algorithms; a real-time approach would be greatly preferable. This is possible; other UEI algorithms are currently being incorporated into high-end, commercially available ultrasound devices (Siemens, GE, Hitachi, Toshiba, etc) with the expectation that UEI will be a useful addition to radiology practice.

The principal limitation of our human study was the lack of a comparison between inflamed and fibrotic intestinal narrowing, which would require resection of the bowel in patients without fibrosis. It would be unethical in human subjects to require resection of stenotic inflammatory bowel for research purposes, so we performed the comparison between intestinal inflammation and fibrosis in rat models. A second limitation is that the measurement of the YM in the grossly normal margins of resected tissue was confounded, because this “normal” tissue contained mild inflammation at a microscopic level. However, this inflammation would be expected to diminish the ability of the YM and UEI to discriminate between stenotic and “normal” bowel.

Similarly, although we made the assumption that the ultrasonographically normal bowel adjacent to stenotic intestine in the human UEI studies was truly normal, it could have been affected by changes related to CD. Again, if inflammation in the apparently “normal” adjacent bowel occurred, this would be expected to reduce the accuracy of UEI. A final limitation of UEI is that, in this study, it was used only to evaluate known stenotic lesions localized on cross-sectional imaging. It would be impractical to use UEI to search the entire bowel for stenoses; UEI will likely be most valuable for the focused evaluation of known lesions. In following CD patients over time, the value of repeated computed tomography enterography is limited by radiation exposure, and the value of repeated magnetic resonance enterography by cumulative cost. For longitudinal monitoring of CD patients at high risk of complications, the combination of contrast- or Doppler-enhanced ultrasonography for the evaluation of intestinal inflammation, and UEI for the evaluation of intestinal fibrosis, could be an attractive option.

Because this was a cross-sectional study, we measured only severe Crohn’s intestinal stenosis requiring surgery. However, our animal model data demonstrate that UEI technology can distinguish intestinal inflammation from fibrosis using transcutaneous ultrasound data. The TNBS-colitis model does induce a T helper-1 cell– driven immune response, but does share important limitations of other animal models of IBD, including mechanistic differences from human CD.[16,17] Although TNBS colitis does not reproduce human CD, it does produce a grossly stiff intestine with histopathologic fibrosis. Because this application of UEI measures intestinal stiffness as a surrogate marker for intestinal fibrosis, the validity of the model depends on the degree of fibrosis and intestinal stiffness, rather than true replication of CD. The finding that UEI can differentiate intestinal fibrosis in CD patients from adjacent normal-appearing bowel supports the validity of the TNBS colitis model. Although the human UEI pilot study was small, it was sufficient to address our aim of determining that UEI scans can be practically performed on human subjects with CD.

Bowel elastography is in its infancy, and the sensitivity and specificity of this approach in humans remains unproven. Future developments in UEI technology, including assessment of the nonlinearity of strain, could improve the discriminant power of UEI for early stages of intestinal fibrosis. We do not yet know how accurate UEI would be for mild, early human intestinal fibrosis, or for following patients (and their stenotic lesions) longitudinally over time. More research is needed to determine whether reduced UEI strain has predictive value, and whether UEI can discriminate between patients likely to respond to anti-inflammatory medical therapy vs those who require operative intervention. These clinically important end points remain to be evaluated in future prospective human studies.

UEI remains far from clinical implementation in IBD, but should it be shown to prospectively differentiate inflammatory from fibrotic changes, this could represent a real-time tool aiding clinical decision making. We speculate that UEI, if prospectively proven, could provide longitudinal information on the natural history of CD, including identifying and longitudinally following high-risk patients who develop early fibrosis and rapidly progress to fibrostenotic strictures. Finally, as a noninvasive means of quantifying fibrosis, UEI could represent an important tool in evaluating candidate anti-fibrotic therapies for CD.

Supplementary Material

Refer to Web version on PubMed Central for supplementary material.

Acknowledgments

Funding

Supported by grants R21-DK081123-01 (KK, JX, PDRH, JMR); K08-DK080172-01 (PDRH), and T32-DK007367-01 (RWS).

Abbreviations used in this paper

CD	Crohn’s disease
IBD	inflammatory bowel disease
PBS	phosphate-buffered saline
RF	radiofrequency
TNBS	trinitrobenzene sulfonic acid
UEI	ultrasound elasticity imaging
YM	Young’s Modulus.

References

1. Loftus EV Jr, Schoenfeld P, Sandborn WJ. The epidemiology and natural history of Crohn’s disease in population-based patient cohorts from North America: a systematic review. Aliment Pharmacol Ther. 2002; 16:51–60. [PubMed: 11856078]
2. Peyrin-Biroulet L, Loftus EV Jr, Colombel JF, et al. The natural history of adult Crohn’s disease in population-based cohorts. Am J Gastroenterol. 2010; 105:289–297. [PubMed: 19861953]

3. Bernstein CN, Nabalamba A. Hospitalization, surgery, and readmission rates of IBD in Canada: a population-based study. Am J Gastroenterol. 2006; 101:110–118. [PubMed: 16405542]
4. Holtmann M, Wanitschke R, Helisch A, et al. [Anti-TNF antibodies in the treatment of inflammatory intestinal stenoses in Crohn's disease]. Z Gastroenterol. 2003; 41:11–17. [PubMed: 12541166]
5. Lichtenstein GR, Olson A, Travers S, et al. Factors associated with the development of intestinal strictures or obstructions in patients with Crohn's disease. Am J Gastroenterol. 2006; 101:1030–1038. [PubMed: 16606351]
6. Ophir J, Cespedes I, Ponnekanti H, et al. Elastography: a quantitative method for imaging the elasticity of biological tissues. Ultrason Imaging. 1991; 13:111–134. [PubMed: 1858217]
7. O'Donnell M, Shapo BM, Emelianov SY. Internal displacement and strain imaging using ultrasonic speckle tracking. IEEE Trans Ultrason Ferroelectr Freq Control. 1994; 41:314–325.
8. Rubin JM, Aglyamov SR, Wakefield TW, et al. Clinical application of sonographic elasticity imaging for aging of deep venous thrombosis: preliminary findings. J Ultrasound Med. 2003; 22:443–448. [PubMed: 12751855]
9. Rubin JM, Xie H, Kim KW, et al. Sonographic elasticity imaging of acute and chronic deep venous thrombosis in humans. J Ultrasound Med. 2006; 25:1179–1186. [PubMed: 16929019]
10. Perk G, Tunick PA, Kronzon I. Non-Doppler two-dimensional strain imaging by echocardiography: from technical considerations to clinical applications. J Am Soc Echocardiogr. 2007; 20:234–243. [PubMed: 17336748]
11. Weitzel WF, Kim K, Rubin JM, et al. Feasibility of applying ultrasound strain imaging to detect renal transplant chronic allograft nephropathy. Kidney Int. 2004; 65:733–736. [PubMed: 14717949]
12. Kim K, Johnson LA, Jia C, et al. Noninvasive ultrasound elasticity imaging (UEI) of Crohn's disease: animal model. Ultrasound Med Biol. 2008; 34:902–912. [PubMed: 18294759]
13. Morris GP, Beck PL, Herridge MS, et al. Hapten-induced model of chronic inflammation and ulceration in the rat colon. Gastroenterology. 1989; 96:795–803. [PubMed: 2914642]
14. Travis SP, Stange EF, Lemann M, et al. European evidence based consensus on the diagnosis and management of Crohn's disease: current management. Gut. 2006; 55(Suppl 1):i16–i35. [PubMed: 16481629]
15. Fraquelli M, Sarno A, Girelli C, et al. Reproducibility of bowel ultrasonography in the evaluation of Crohn's disease. Dig Liver Dis. 2008; 40:860–866. [PubMed: 18583205]
16. Camoglio L, te Velde AA, de Boer A, et al. Hapten-induced colitis associated with maintained Th1 and inflammatory responses in IFN-gamma receptor-deficient mice. Eur J Immunol. 2000; 30:1486–1495. [PubMed: 10820397]
17. te Velde AA, Verstege MI, Hommes DW. Critical appraisal of the current practice in murine TNBS-induced colitis. Inflamm Bowel Dis. 2006; 12:995–999. [PubMed: 17012970]

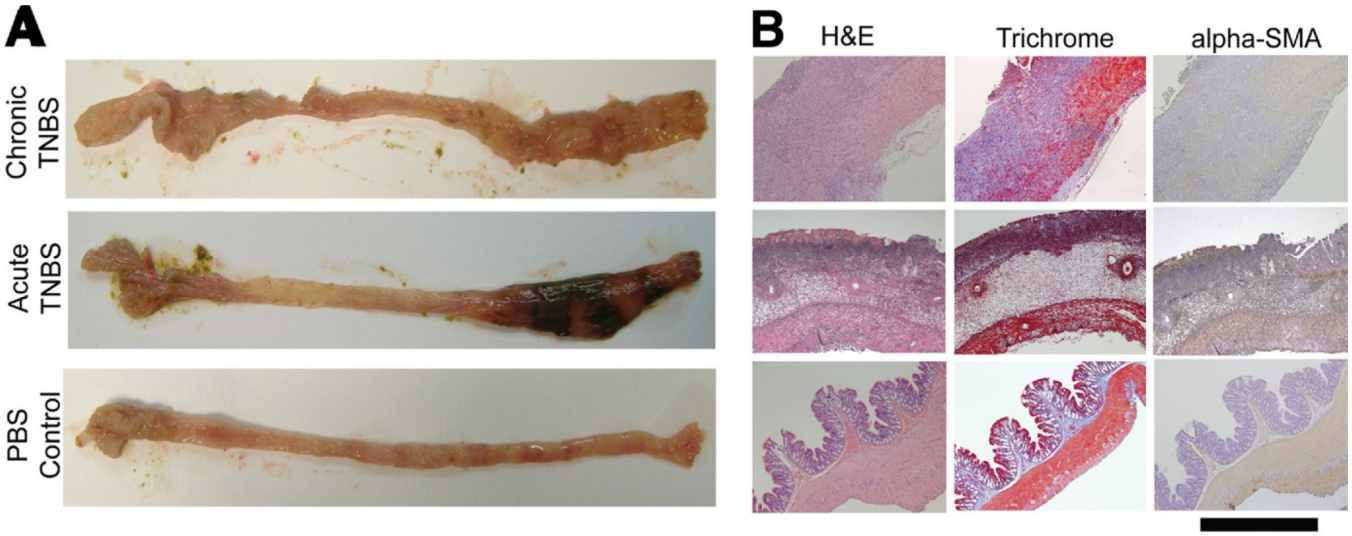

C

Animal Histologic Scoring														
	PBS (n=3)			Chronic TNBS (n=6)						Acute TNBS (n=5)				
Fibrosis	0	0	0	3	3	3	2	3	3	0	0	0	0	0
Inflammation	0	0	0	2	2	2	1	2	2	3	3	3	3	3
MM Thickening	No	No	No	Yes	Yes	Yes	Yes	Yes	Yes	No	No	No	No	No
Ulceration	No	No	No	Yes	Yes	Yes	No	Yes	Yes	Yes	Yes	Yes	Yes	Yes
Necrosis	No	No	No	No	No	No	No	No	No	Yes	Yes	Yes	Yes	Yes

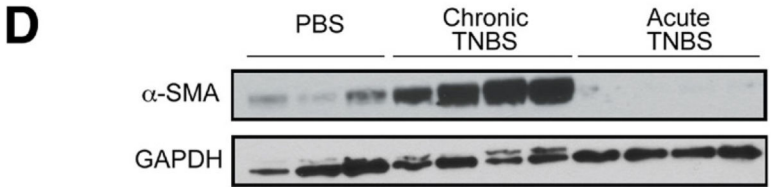

Figure 1.

Acute and chronic TNBS enemas generate colitis and colonic fibrosis, respectively, in Lewis rats. (*A*) Gross analysis reveals thickened and stiff distal colon segments in the chronically treated group (*upper panel*), whereas gross edema, hemorrhage, necrosis, and soft tissue is found in the acute colitis group (*middle panel*). The PBS-treated rats and the proximal colon segments in all groups (not reached by the enemas) were grossly unaffected (*lower panel*). (*B*) The histology of distal colon sections shows predominantly fibrotic changes in the chronic TNBS rats with extensive submucosal thickening due to increased extracellular matrix deposition, as shown by Masson's trichrome staining of collagen (*blue*) and marked muscularis mucosa (*MM*) thickening as seen by α-SMA staining (original magnification, ×50). Predominantly inflammatory changes without fibrosis were seen in the acute treatment model. Histologic scoring in all animals is detailed in the accompanying table. (*C*) Western blotting of colonic extracts for α-SMA. GAPDH protein expression was used as a loading control.

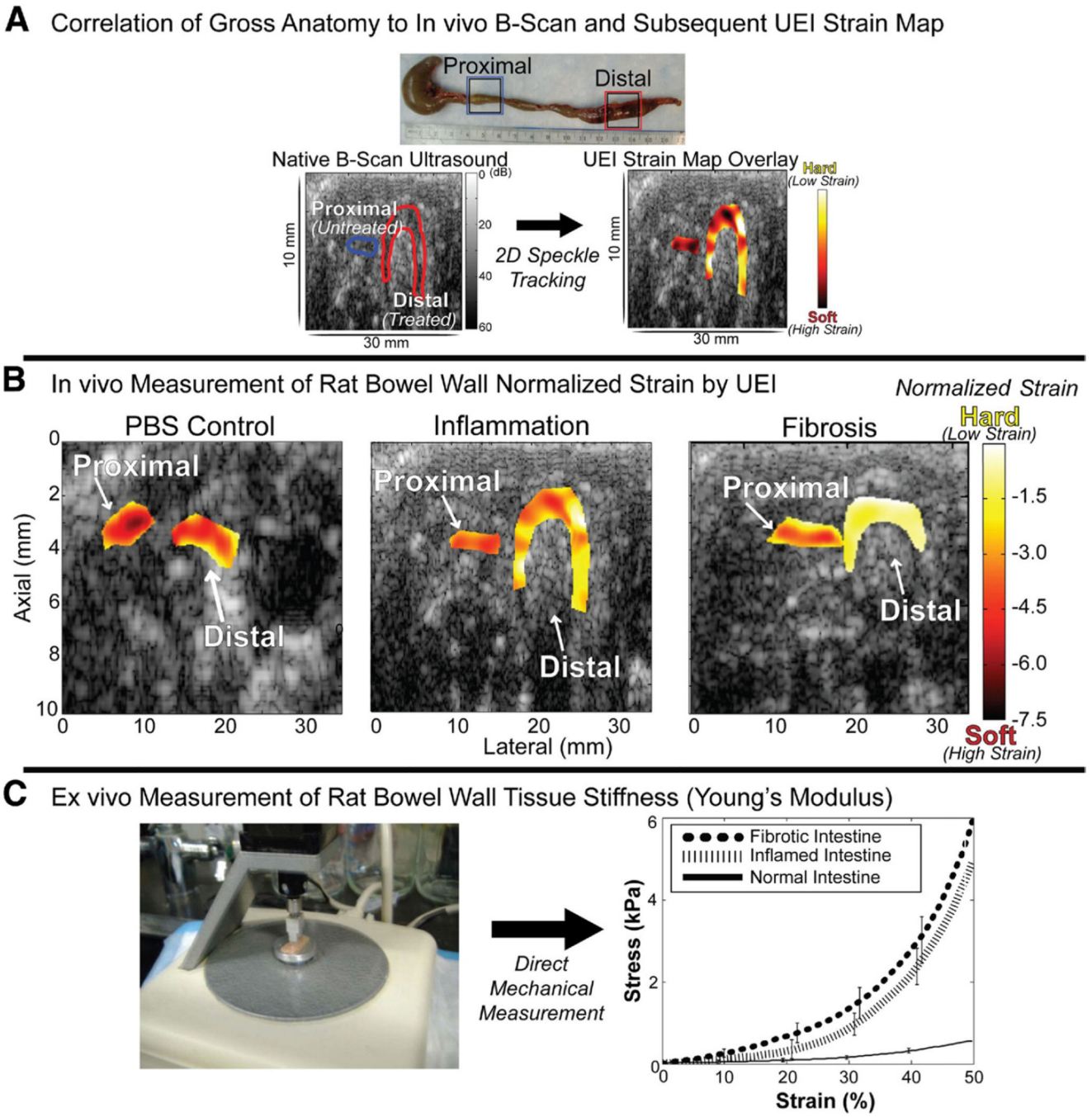

Figure 2.

(*A*) Female Lewis rats received enemas of TNBS-50% ethanol or PBS control enemas; measurements of the affected distal colon segment are compared with proximal segment, acting as an intra-animal control. Using the transducer for compression, transabdominal ultrasound RF data is collected and a region of interest is selected (bowel wall) for 2-dimensional speckle tracking. (*B*) UEI normalized strain maps for PBS enemas (negative control group), acute TNBS enemas (acute inflammation group), and chronic weekly TNBS enemas (intestinal fibrosis group) in Lewis rats. The proximal colons in all animals (not

reached by enemas) had similar UEI strain estimates. Fibrotic colon had the lowest mean strain (hardest), measuring −1.10 ± 0.167. PBS-treated (negative control) distal colon had the highest mean normalized strain (softest) of −3.57 ± 0.352. The acute inflammatory colitis group had an intermediate mean normalized strain value of −2.07 ± 0.717. Normalized strain values differentiated normal from diseased bowel ($P = .015$). Normalized strain also differentiated acute colitis and chronic fibrosis groups ($P = .037$), suggesting that UEI can distinguish intestinal inflammation from intestinal fibrosis in Lewis rats. (*C*) Tissue mechanical properties were assessed using a microelastometer. Fibrotic tissue had the highest YM (stiffest) 3.44 ± 1.50 kPa; normal tissue had the lowest YM (softest) 1.03 ± 0.15 kPa; and inflammatory tissue had intermediate stiffness of 2.50 ± 0.70 kPa. These values were normalized to the right colon measurement of YM, and the paired differences between all 3 groups were statistically significant fibrotic versus inflamed ($P = .024$), inflamed versus control ($P = .042$), and fibrotic versus control ($P = .035$). Averaged stress–strain curves with *errors bars* showing standard deviation.

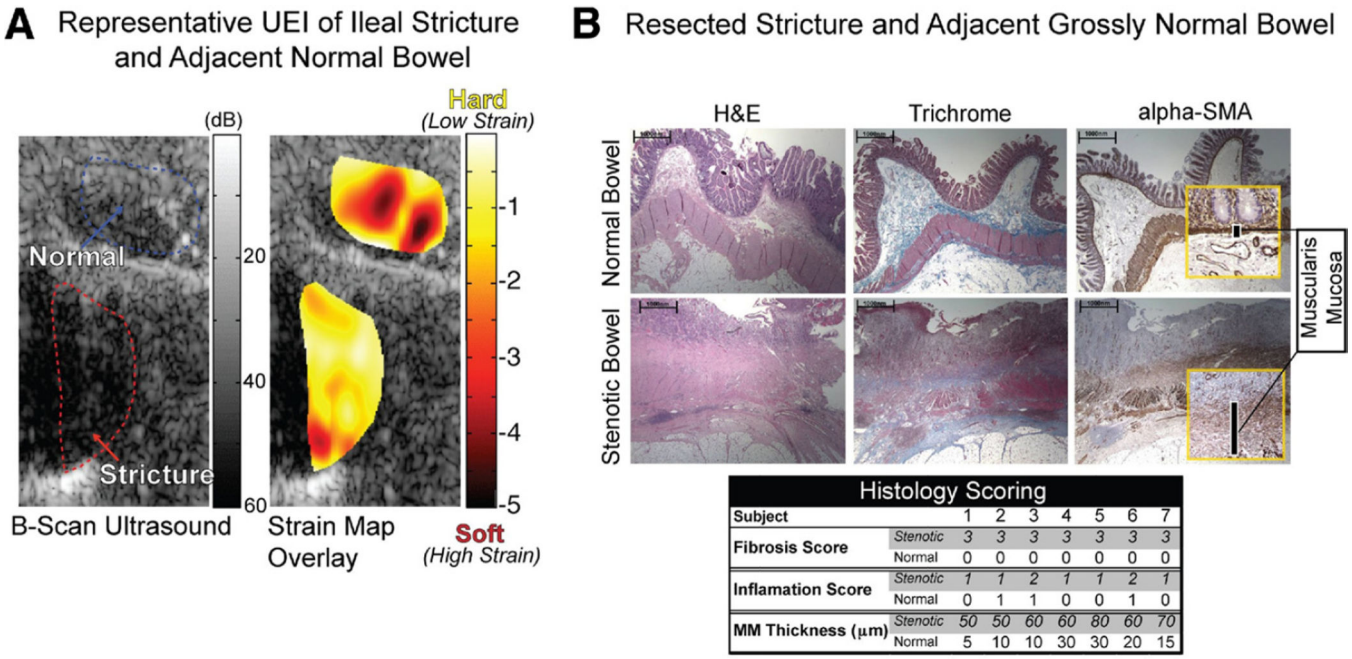

Histology Scoring

Subject		1	2	3	4	5	6	7
Fibrosis Score	*Stenotic*	*3*	*3*	*3*	*3*	*3*	*3*	*3*
	Normal	0	0	0	0	0	0	0
Inflamation Score	*Stenotic*	*1*	*1*	*2*	*1*	*1*	*2*	*1*
	Normal	0	1	1	0	0	1	0
MM Thickness (μm)	*Stenotic*	*50*	*50*	*60*	*60*	*80*	*60*	*70*
	Normal	5	10	10	30	30	20	15

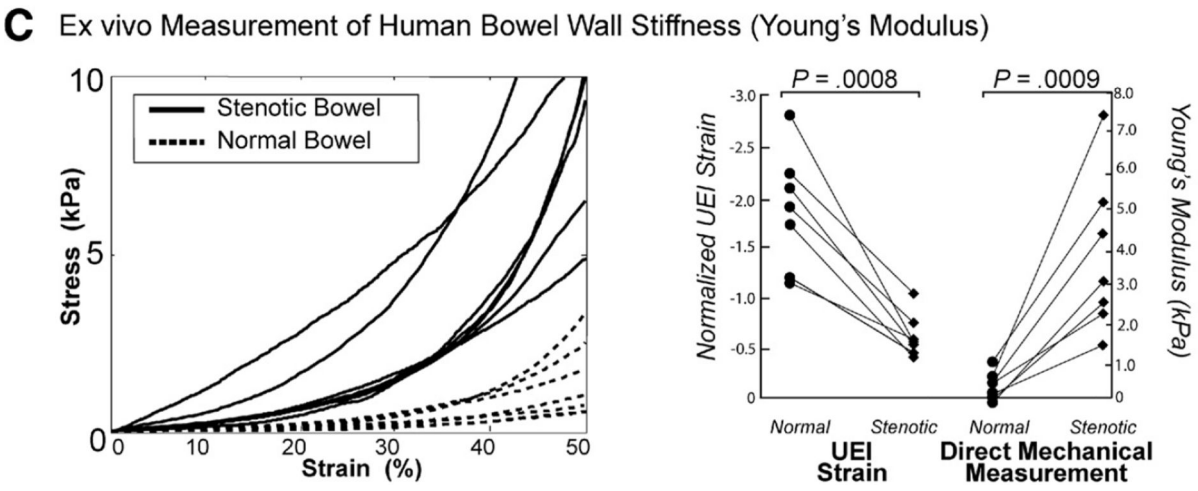

Figure 3.

(*A*) Representative ultrasound B-scan image of a CD subject with symptomatic small bowel stricture, outlining the regions of interest (*ROI*) for the stricture and adjacent normal-appearing bowel in B-Scan mode (*left panel*). The corresponding UEI normalized strain map is presented (*right panel*). Across 7 subjects, the mean UEI normalized strain in stenotic bowel was −0.87 ± 0.22. Adjacent normal-appearing bowel was significantly softer (−1.99 ± 0.53; $P = .0008$). (*B*) Histology of normal human bowel from resected margins, compared with stenotic human bowel stained with hematoxylin and eosin, Masson's trichrome, and α-SMA (original magnification, ×5). *Inset* (original magnification, ×50) details changes in the muscularis mucosa thickness (*vertical black bar*). Histology scoring of each subject shown in the accompanying table. (*C*) Direct mechanical measurement of tissue samples from Crohn's subjects, plotted as stress vs strain, revealed fibrostenotic sections of bowel were clearly more stiff (mean YM 4.14 ± 1.88 kPa) than the grossly normal tissue resection

margins (mean YM 0.96 ± 0.25 kPa) in all subjects ($P = .0009$; *left panel*). Strain and stress are inversely proportional mechanical properties, with low strain and high stress both indicating stiffness (hardness). Plotting UEI strain and YM of normal and stenotic bowel with lines connecting individual subjects, UEI strain and direct mechanical measurement are appropriately inversely correlated ($r = -0.81$; *right panel*). The noninvasive transcutaneous UEI measurements are accurate estimates of the true tissue mechanical properties of intestine.